THE JOURNAL OF BIOLOGICAL CHEMISTRY VOL. 286, NO. 20, pp. 17945–17953, May 20, 2011

Controlling the Activity of a Phosphatase and Tensin Homolog (PTEN) by Membrane Potential*

Received for publication, November 8, 2010, and in revised form, February 21, 2011 Published, JBC Papers in Press, March 17, 2011, DOI 10.1074/jbc.M110.201749

Jérôme Lacroix[‡1], Christian R. Halaszovich[§1], Daniela N. Schreiber[§], Michael G. Leitner[§], Francisco Bezanilla[‡], Dominik Oliver[§2], and Carlos A. Villalba-Galea[¶3]

From the [‡]Department of Biochemistry and Molecular Biology, The University of Chicago, Chicago, Illinois 60637, the [§]Institute of Physiology and Pathophysiology, Philipps University, 35037 Marburg, Germany, and the [¶]Department of Physiology and Biophysics, Virginia Commonwealth University, Richmond, Virginia 23298

The recently discovered voltage-sensitive phosphatases (VSPs) hydrolyze phosphoinositides upon depolarization of the membrane potential, thus representing a novel principle for the transduction of electrical activity into biochemical signals. Here, we demonstrate the possibility to confer voltage sensitivity to cytosolic enzymes. By fusing the tumor suppressor PTEN to the voltage sensor of the prototypic VSP from *Ciona intestinalis*, Ci-VSP, we generated chimeric proteins that are voltage-sensitive and display PTEN-like enzymatic activity in a strictly depolarization-dependent manner *in vivo*. Functional coupling of the exogenous enzymatic activity to the voltage sensor is mediated by a phospholipid-binding motif at the interface between voltage sensor and catalytic domains. Our findings reveal that the main domains of VSPs and related phosphoinositide phosphatases are intrinsically modular and define structural requirements for coupling of enzymatic activity to a voltage sensor domain. A key feature of this prototype of novel engineered voltage-sensitive enzymes, termed Ci-VSPTEN, is the novel ability to switch enzymatic activity of PTEN rapidly and reversibly. We demonstrate that experimental control of Ci-VSPTEN can be obtained either by electrophysiological techniques or more general techniques, using potassium-induced depolarization of intact cells. Thus, Ci-VSPTEN provides a novel approach for studying the complex mechanism of activation, cellular control, and pharmacology of this important tumor suppressor. Moreover, by inducing temporally precise perturbation of phosphoinositide concentrations, Ci-VSPTEN will be useful for probing the role and specificity of these messengers in many cellular processes and to analyze the timing of phosphoinositide signaling.

Many cellular processes, ranging from secretion of hormones and neurotransmitters to gene transcription, can be triggered by rapid changes in membrane potential. The canonical principle for transduction of membrane potential changes into intracellular signals involves Ca^{2+} influx by activation of voltage-gated channels, resulting in an increase of the intracellular Ca^{2+} concentration, which in turn acts via downstream Ca^{2+}-sensitive proteins as effectors (1–3). The recent discovery of voltage-sensitive phosphatases (VSPs)[4] (4, 5) has broadened this view fundamentally. In response to depolarization of the membrane potential, the prototypic VSP from *Ciona intestinalis*, Ci-VSP (5, 6), degrades both phosphatidylinositol 4,5-bisphosphate ($PI(4,5)P_2$) and phosphatidylinositol 3,4,5-trisphosphate ($PI(3,4,5)P_3$) by removing the phosphate group in position 5 of the inositol ring (5–8). These phosphoinositides are signaling molecules with pivotal roles in the regulation of various cellular processes such as cell proliferation and differentiation (9, 10), ion channel activity (11), synaptic exocytosis and endocytosis (12, 13), and neural development (9). Thus, VSPs constitute a novel mechanism of coupling of intracellular pathways to electrical activity at the plasma membrane, although their physiological role remains elusive.

VSPs are homologues of the tumor suppressor PTEN (phosphatase and tensin homolog deleted from chromosome 10) (14, 15), a key regulator of phosphoinositide signaling pathways. PTEN is a cytosolic 3′-phosphoinositide phosphatase, acting as an antagonist of the Akt/PI3K pathway. Loss-of-function mutations of PTEN are frequently found in human cancer, ranking this protein as one of the most important tumor suppressors known presently (16). Regulation of PTEN activity is highly complex, but in contrast to VSPs, it is independent of membrane potential because PTEN is a cytosolic protein. Because the membrane lipid $PI(3,4,5)P_3$ is the main substrate of PTEN, binding to the plasma membrane is a prerequisite for enzymatic activity. Targeting to the plasma membrane is mediated by two distinct domains located in the N and C termini (17–20). The C terminus harbors a C2 domain that binds phosphatidylserine; its binding affinity is regulated by phosphorylation (19, 21). The N terminus constitutes a phosphoinositide-binding motif (PBM) that recruits PTEN to the membrane by specifically binding to $PI(4,5)P_2$, the main catalytic product of PTEN (17, 22). Moreover, binding of the PBM to $PI(4,5)P_2$ allosterically activates PTEN (17, 22). Thus, the activity of PTEN relies not

* This work was supported, in whole or in part, by National Institutes of Health Grant GM030376 (to F. B.). This work was also supported by Deutsche Forschungsgemeinschaft Grant SFB593 TPA12 (to D. O.).

[1] Both authors contributed equally to this work.

[2] To whom correspondence may be addressed: Institut für Physiologie und Pathophysiologie, Deutschhausstr. 1-2, 35037 Marburg, Germany. Fax: 49-6421-2862306; E-mail: oliverd@staff.uni-marburg.de.

[3] To whom correspondence may be addressed: Department of Physiology and Biophysics, 1101 E. Marshall St., Richmond, VA 23298. Fax: 1-804-828-7382; E-mail: cavillalbaga@vcu.edu.

[4] The abbreviations used are: VSP, voltage-sensitive phosphatase; CD, catalytic domain; OK, opossum kidney; PBM, phosphoinositide binding motif; PD, phosphatase domain; PH, pleckstrin homology domain; $PI(4,5)P_2$, phosphatidylinositol(4,5)bisphosphate; $PI(3,4)P_2$, phosphatidylinositol(3,4)bisphosphate; $PI(3,4,5)P_2$, phosphatidylinositol(3,4,5)trisphosphate; PI(4)P, phosphatidylinositol 4-phosphate.

only on the recognition of its substrate but also on binding to the membrane and on a membrane-delimited allosteric interaction with $PI(4,5)P_2$, which acts as an activating ligand. This complexity poses substantial challenges for further detailed examination of the mechanism of activation, enzymatic mechanism, and regulation of PTEN and of its multiple cellular functions (23). A robust method for experimental control of PTEN activity, analogous to the voltage control of the VSPs, might therefore greatly facilitate such examination.

In VSPs, voltage sensitivity is conferred by a voltage-sensing domain (VSD) located in the N terminus, which, in turn, controls the activity of the catalytic domain (CD) located within the C terminus (see Fig. 1*A*). Both domains are fully functional when expressed individually (5, 24). The modular nature of both domains suggested that the VSD initiates the catalytic activity by operating a molecular switch intrinsic to the CD. The N terminus of the CD of Ci-VSP also contains a PBM highly homologous to the PBM of PTEN (see Fig. 1*B*), which is critical for depolarization-triggered activity. In fact, it has been proposed that the mechanism of activation of the Ci-VSP involves binding of the PBM to the membrane (8, 24); accordingly, voltage sensitivity relies on the control of this binding step by the VSD. Thus, activation of VSPs resembles the PBM-mediated activation of PTEN. Moreover, the CD of Ci-VSP shares substantial sequence conservation with PTEN (8, 25). A structural homology model for the CD of Ci-VSP (see Fig. 1*C*) based upon the crystal structure of PTEN as a template (26) confirmed a high degree of structural similarity between Ci-VSP and PTEN, including an architecture consisting of a phosphatase domain (PD) and a C2 domain. These considerations suggested that it may be possible to impose voltage control upon PTEN if it was connected properly to a VSD. Following this idea, we here describe the successful generation and characterization of engineered voltage-activated enzymes (VEnz), by conferring voltage sensitivity upon the cytoplasmic signaling enzyme PTEN.

EXPERIMENTAL PROCEDURES

Generation of Ci-VSPTEN Chimera and Mutagenesis—Ci-VSPTEN chimeras were built by swapping the DNA fragments encoding the codons 240–576 (Ci-VSPTEN0), 255–576 (Ci-VSPTEN16), and 260–576 (Ci-VSPTEN21) of Ci-VSP by the DNA fragments encoding the codons 1–403 (Ci-VSPTEN0), 16–403 (Ci-VSPTEN16), and 21–403 (Ci-VSPTEN21) of the mouse PTEN cDNA.[5] For this, we employed a PCR-based primer extension strategy. Briefly, the PTEN DNA fragments were generated by PCR-amplification from a Sport6 plasmid containing the full-length PTEN cDNA. The 5′ ends of the sense and antisense primers used for these PCR were complementary to the 5′ and 3′ regions immediately flanking the sequence to swap in the Ci-VSP cDNA. The obtained PCR products were purified and used as extended primers for a second PCR reaction using a standard QuikChange mutagenesis protocol (Stratagene). The DNA template used for these second PCR was a pBSTA plasmid encoding the Ci-VSP cDNA under the T7 promoter. For expression in CHO and opossum kidney (OK) cells, Ci-VSPTEN chimeras were subcloned from pBSTA into pRFP-C1. Ci-VSPTEN mutants were generated by standard site-directed mutagenesis and verified by sequencing. Sensing current recordings and voltage clamp fluorometry, were performed with Ci-VSPTEN containing the additional mutation C363S, equivalent to the catalytically inactive mutant C124S in PTEN.

Expression in Xenopus Oocytes—The DNA was linearized with NotI and transcribed using T7 RNA polymerase. 50 nl of 0.5–1 μg/μl RNA was injected per oocyte, followed by incubation at 18 °C in a solution containing 100 mM NaCl, 2 mM KCl, 1 mM $MgCl_2$, 1.8 mM $CaCl_2$, 2 mM sodium pyruvate, 50 μM EDTA, and 10 mM HEPES, pH 7.5 (27).

Sensing Currents and Voltage Clamp Fluorometry—Sensing currents were measured 2–4 days after injection with the cut-open oocyte voltage clamp technique (28) as described by Villalba-Galea *et al.* (27). Currents were measured in response to voltage steps (400 ms, 10-s interval) from a holding potential of −80 mV without leak subtraction during acquisition. Capacitance transient currents were compensated analogically using the amplifier compensation circuit. The external recording solutions contained 120 mM NMG-$MeSO_3$ (methanesulfonate), 10 mM HEPES, and 2 mM $CaCl_2$, pH 7.4, whereas internal solutions contained 120 mM NMG-$MeSO_3$, 10 mM HEPES, and 2 mM EGTA, pH 7.4. Labeling of oocytes with tetramethylrhodamine-5-maleimide and fluorometry were done as described previously (29). Briefly, tetramethylrhodamine-5-maleimide fluorescence was measured through a BX51WI microscope (Olympus) equipped with a LUMPlanFl 40× water immersion objective (numerical aperture, 0.80) and an appropriate filter set. Fluorescence intensity was monitored with a PhotoMax-201-PIN photodiode controlled by a PhotoMax 200 amplifier (Dagan). Electrophysiological and fluorescence data were filtered at 2–5 kHz and sampled at 5–20 kHz and recorded and analyzed with the acquisition system and programs described previously (27).

Expression in CHO and OK Cells—CHO and OK cells were grown as described (7, 30), plated onto glass-bottomed dishes (WillCo Wells B. V., Amsterdam, The Netherlands) or glass coverslips, respectively, and transfected using jetPEI (CHO cells; Polyplus Transfection, Illkirch, France) or Lipofectamine 2000 (OK cells; Invitrogen). Experiments were done 24–48 h post-transfection on cells selected for expression of mRFP-Ci-VSPTEN and the presence of corresponding sensing currents. Vectors used for transfection were as follows: PLCδ1-PH-pEGFP-N1 (GenBank accession no. P51178); Akt1-PH-pEGFP-N1 (GenBank accession no. AAL55732.1); Btk-PH-pEGFP (GenBank accession no. AAC51347.1); OSBP-PH-pEGFP-N1 (GenBank accession no. NP_002547.1); TAPP1-PH-FUGW (GenBank accession no. NP_067635); bovine phosphatidylinositol 3-kinase p110α (constitutively active mutant K227E; GenBank accession no. NP_776999.1); and hTASK-3-pcDNA3.1 (GenBank accession no. NP_057685).

Combined Patch Clamp and TIRF Microscopy—CHO cells were whole-cell voltage clamped with an EPC-10 amplifier con-

[5] PTEN from both human and mouse displays 96% identity in their nucleotide sequence, while only differing in a single amino acid in the distal region of the C terminus, particularly a Serine in position 398, instead of a Threonine, as in human. To our knowledge, there is no evidence showing any difference between the activities of these two enzymes.

trolled by PatchMaster software (HEKA, Lambrecht, Germany). Sensing currents were isolated using a P/-10 protocol. Patch pipettes were pulled from a quartz glass to an open pipette resistance of 1.5–4.0 MΩ when filled with intracellular solution: 135 mM KCl, 2.5 mM $MgCl_2$, 2.41 mM $CaCl_2$, 5 mM EGTA, 5 mM HEPES, and 3 mM Na_2ATP, pH 7.3 (with KOH). For perforated patch measurements Nystatin (100 μg/ml) was added. The extracellular solution contained the following: 144 mM NaCl, 5.8 mM KCl, 0.7 mM NaH_2PO_4, 5.6 mM glucose, 1.3 mM $CaCl_2$, 0.9 mM $MgCl_2$, and 10 mM HEPES, pH 7.4 (with NaOH). For depolarization by K^+, cells were initially kept in standard extracellular solution, and depolarization was induced by transient application of 150 mM K^+ (150 mM KCl, 5.6 mM glucose, 1.3 mM $CaCl_2$, 0.9 mM $MgCl_2$, and 10 mM HEPES, pH 7.4). Total internal reflection fluorescence (TIRF) imaging was done as described previously (7). Briefly, a BX51WI upright microscope (Olympus) equipped with a TIRF condenser (numerical aperture, 1.45; Olympus) and a 488-nm laser (20 milliwatt; Picarro, Sunnyvale, CA) was used. Fluorescence was imaged through a LUMPlanFI/IR 40×/0.8 numerical aperture water-immersion objective. Images were acquired with a TILL-Imago QE cooled CCD camera (TILL Photonics, Gräfelfing, Germany) controlled by TILLvision software (TILL Photonics). Imaging data were analyzed using TILLvisION and IgorPro (Wavemetrics, Lake Oswego, OR). Regions of interest encompassed the footprint of a single cell excluding cell margins to avoid movement artifacts. F/F_0 traces were calculated from the background-corrected TIRF signal intensity F, averaged over the region of interest and the initial fluorescence intensity F_0 during the baseline interval. F/F_0 traces were corrected for bleaching according to monoexponential fits to the baseline interval.

Confocal Imaging—OK cells were co-transfected with mRFP-Ci-VSPTEN16, Akt-PH-GFP, p110α(K227E), and the TASK3 potassium channel. Cells were transiently depolarized by application of 150 mM K^+. Confocal imaging was performed with a Zeiss Examiner upright microscope equipped with a LSM710 scan head (Carl Zeiss AG, Jena, Germany) and a W-Plan-Apochromat 20×/1.0 DIC M27 75 mm (Carl Zeiss AG). Laser lines used were 561 nm for mRFP and 488 nm for GFP, detection wavelength ranges were 582–754 and 493–582 nm, respectively. Time series recordings were taken in the GFP channel. Fluorescence (F) was averaged from regions of interest placed in cytosolic regions of individual cells and normalized to the baseline fluorescence (F_0), prior to stimulation.

All experiments were performed at room temperature. Data are given as means ± S.E.

RESULTS

Designing Chimeras between Ci-VSP and PTEN—A chimera, hereafter named Ci-VSPTEN16, was built by replacing the CD of Ci-VSP with full-length PTEN (Fig. 1*D*). Because the PBM is critically involved in mediating activation both in Ci-VSP and PTEN, we particularly focused our attention on the motif linking PTEN to the VSD in the chimeras. Previous functional analysis showed that, in Ci-VSP, the VSD seems to control the binding of the PBM to the membrane, and this process is critically dependent on arginines 253 and 254. In fact, mutation of these

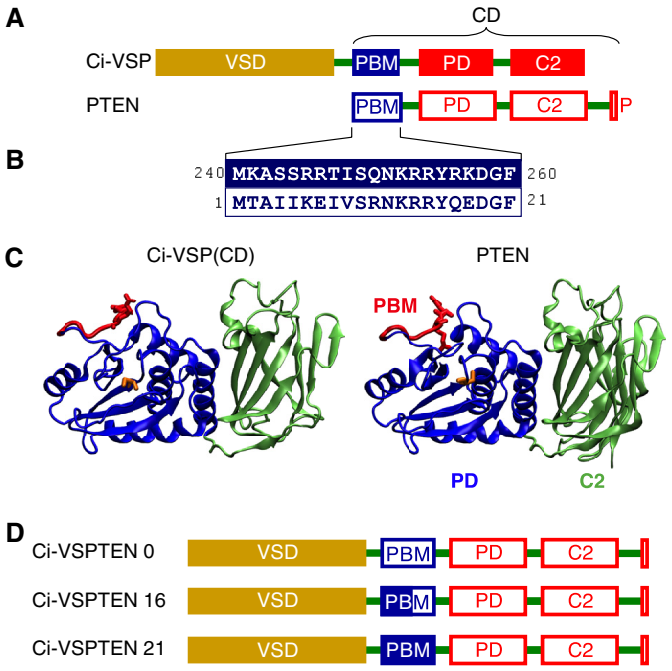

FIGURE 1. **Design of chimeras between Ci-VSP and PTEN.** *A*, comparison of the domain organization of Ci-VSP and PTEN. *P*, PDZ-binding motif. *B*, high sequence identity between the PBMs of Ci-VSP and PTEN. *Numbers* refer to the amino acid positions in Ci-VSP and PTEN, respectively. *C*, structural similarity between the catalytic domains of Ci-VSP and PTEN predicted by structural homology modeling of the CD of Ci-VSP (*left panel*) based on the crystal structure of PTEN (26), generated with ESyPred3D (48). PD and C2 domains are displayed in *blue* and *green*, respectively. Partially rendered PBMs are shown in *red*, with arginines 253 and 254 in Ci-VSP and arginines 14 and 15 in PTEN emphasized as *stick* models. Cysteines 363 (in Ci-VSP) and 124 (in PTEN) in the catalytic core are displayed as *yellow stick* models. *D*, design of Ci-VSPTEN chimeras. PTEN replaces the CD of Ci-VSP with different variants of the PBM (see text).

arginines eliminates coupling between electrical and catalytic activity (8, 24) even if the charges are conserved (8). In addition, arginines 245 and 246 are also critical for coupling since neutralization of these residues renders coupling inefficient (8). Despite overall similarity, the PBM of PTEN lacks the arginines equivalent to 245 and 246 of Ci-VSP, displaying no net charge at the corresponding position (Fig. 1*B*). To account for potential relevance of these residues for coupling of PTEN to the VSD, we replaced the DNA sequence coding from amino acid 17 of the PBM from Ci-VSP (including $Arg^{245/246}$), with the coding sequence of PTEN contributing the more distal part of the PBM (Ci-VSPTEN16; see Fig. 1, *B* and *D*).

In addition to positions $Arg^{245/246}$, there are further differences in the sequences of the PBMs from Ci-VSP and PTEN (see Fig. 1*B*), which may be relevant for coupling between VSD and PD. In fact, some of these amino acids are known to have a critical impact on the function of PTEN (18, 20, 31). To account for a potential impact of these residues on electrochemical coupling, we designed two additional chimeras containing either the full-length PBM (*i.e.* 21 residues) of Ci-VSP (termed Ci-VSPTEN21) or the full PBM of PTEN without contribution from the PBM of Ci-VSP (Ci-VSPTEN0) (see Fig. 1*D*).

Ci-VSPTEN16 Displays Voltage-activated Enzymatic Activity—Enzymatic activity of Ci-VSPTEN16 was assessed in living cells by imaging genetically encoded fluorescent phosphoinositide probes, following paradigms established previously for Ci-VSP

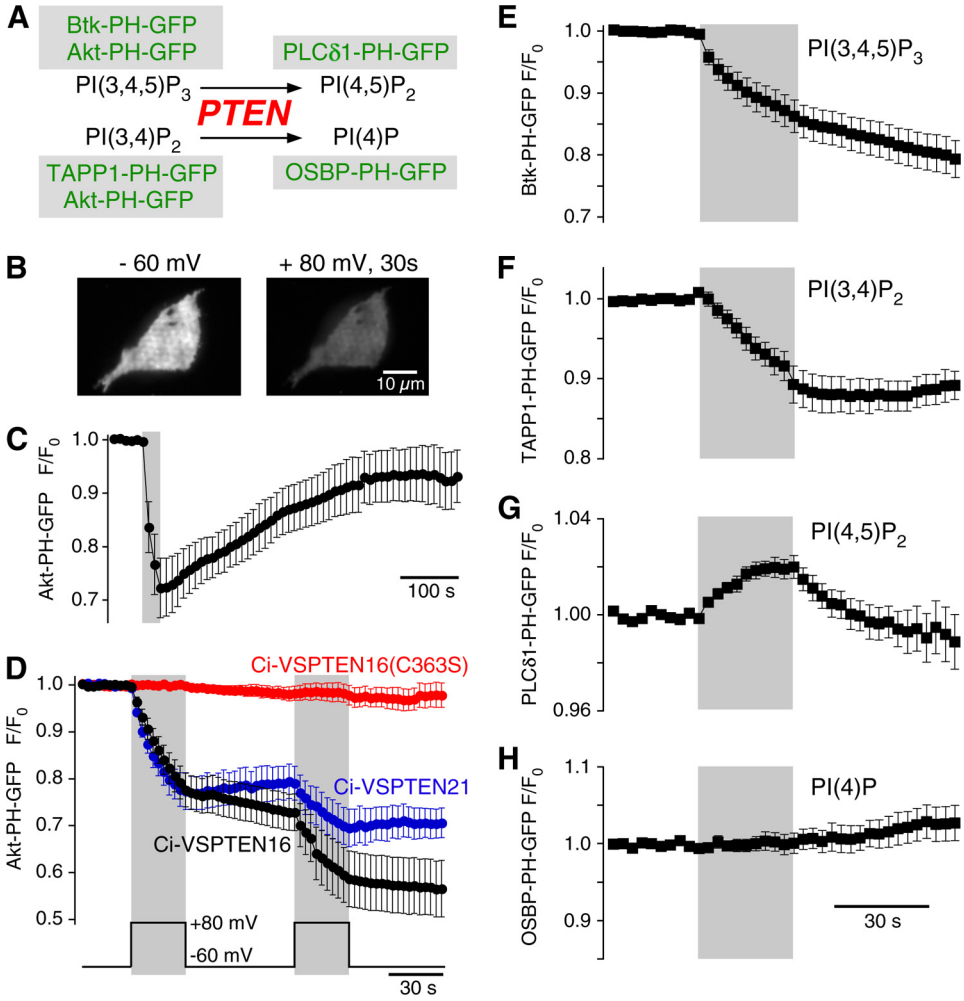

FIGURE 2. **Ci-VSPTEN displays voltage-activated lipid phosphatase activity.** *A*, schematic representation of the enzymatic activity of PTEN, a 3′-phosphatase that converts PI(3,4,5)P_3 into PI(4,5)P_2 and PI(3,4)P_2 into PI(4)P. GFP-fused sensor domains used in this study to detect concentration changes of the putative substrates and products of Ci-VSPTEN chimeras are indicated (*green*). *B*, TIRF images of a living CHO cell coexpressing the PI(3,4,5)P_2/PI(3,4)P_2 sensor Akt-PH-GFP and Ci-VSPTEN16 together with constitutively active PI3K p110αK227E (*PI3K*). Images were acquired before (*left*) and after 30 s of depolarization to +80 mV (*right*) in whole-cell configuration. Depolarization-induced loss of fluorescence results from reduced membrane association of Akt-PH and indicates depletion of 3′-phosphoinositides. *C*, depolarization-induced translocation of Akt-PH as in *B* is followed by slow recovery, indicating resynthesis of 3′-phosphoinositides by PI3K (recordings obtained with perforated patch configuration). The *gray* area indicates depolarization from −60 to +80 mV. *D*, normalized TIRF intensities in response to repetitive depolarization obtained as in *B*. Cells coexpressed Akt-PH-GFP, PI3K, and the Ci-VSPTEN chimeras indicated (n = 10, 3, and 7 cells, for Ci-VSPTEN16, Ci-VSPTEN21, and Ci-VSPTEN16-C363S, respectively). *E–H*, depolarization-triggered changes in membrane association of fluorescent probes that specifically bind various phosphoinositides, measured as in *D*. Cells expressed Ci-VSPTEN16 together with PI3K and either Btk-PH-GFP (n = 16), TAPP1-PH-GFP (n = 5), PLCδ1-PH-GFP (n = 6), or OSBP-PH-GFP (n = 6). *Error bars* indicate S.E.

(7). Briefly, membrane association of these probes reports the abundance of the specifically recognized lipid. Membrane association was determined by TIRF imaging of cells under whole-cell voltage clamp.

Upon depolarization (to +80 mV), cells co-expressing Ci-VSPTEN16 and the probe Akt-PH-GFP, specific for PI(3,4,5)P_3 and PI(3,4)P_2, displayed an unambiguous decrease in membrane-associated fluorescence intensity (Fig. 2, *B* and *C*). This observation showed that the concentration of PI(3,4,5)P_3 and/or PI(3,4)P_2 decreased during depolarization, indicating that Ci-VSPTEN16 has depolarization-triggered enzymatic activity. Following repolarization, the membrane-associated fluorescence recovered, indicating resynthesis of PI(3,4,5)P_3 and/or PI(3,4)P_2 (Fig. 2*C*). Activation of Ci-VSPTEN16 was rapidly reversible, as fluorescence decrease was observed only during depolarization and ceased upon repolarization to −60 mV, as demonstrated using double-pulse protocols (Fig. 2*D*). Similar results were obtained with Ci-VSPTEN21 but not with the catalytically inactive mutant Ci-VSPTEN16-C363S (this mutation is equivalent to C124S in PTEN) (Fig. 2*C*), confirming that the fluorescence decrease was caused by enzymatic activity of the PTEN domain of the chimeras.

The decrease in Akt-PH-GFP TIRF fluorescence obtained with Ci-VSPTEN16 after 60 s of depolarization (+80 mV) was to 46.8 ± 7.2% of the initial signal (n = 5). Because a signal decrease to ~40% reports the full translocation of an initially fully membrane-resident probe (7), this finding indicates that Ci-VSPTEN16 can completely deplete the pool of PI(3,4,5)P_3 and PI(3,4)P_2 in the plasma membrane.

Ci-VSPTEN16 Preserves PTEN Substrate Selectivity—Having found that Ci-VSPTEN16 is both active and voltage-dependent, we next examined the catalytic specificity of this chimera using other phosphoinositide-specific probes (Fig. 2*A*). When co-expressed with Btk-PH-GFP or TAPP1-PH-GFP (32), which

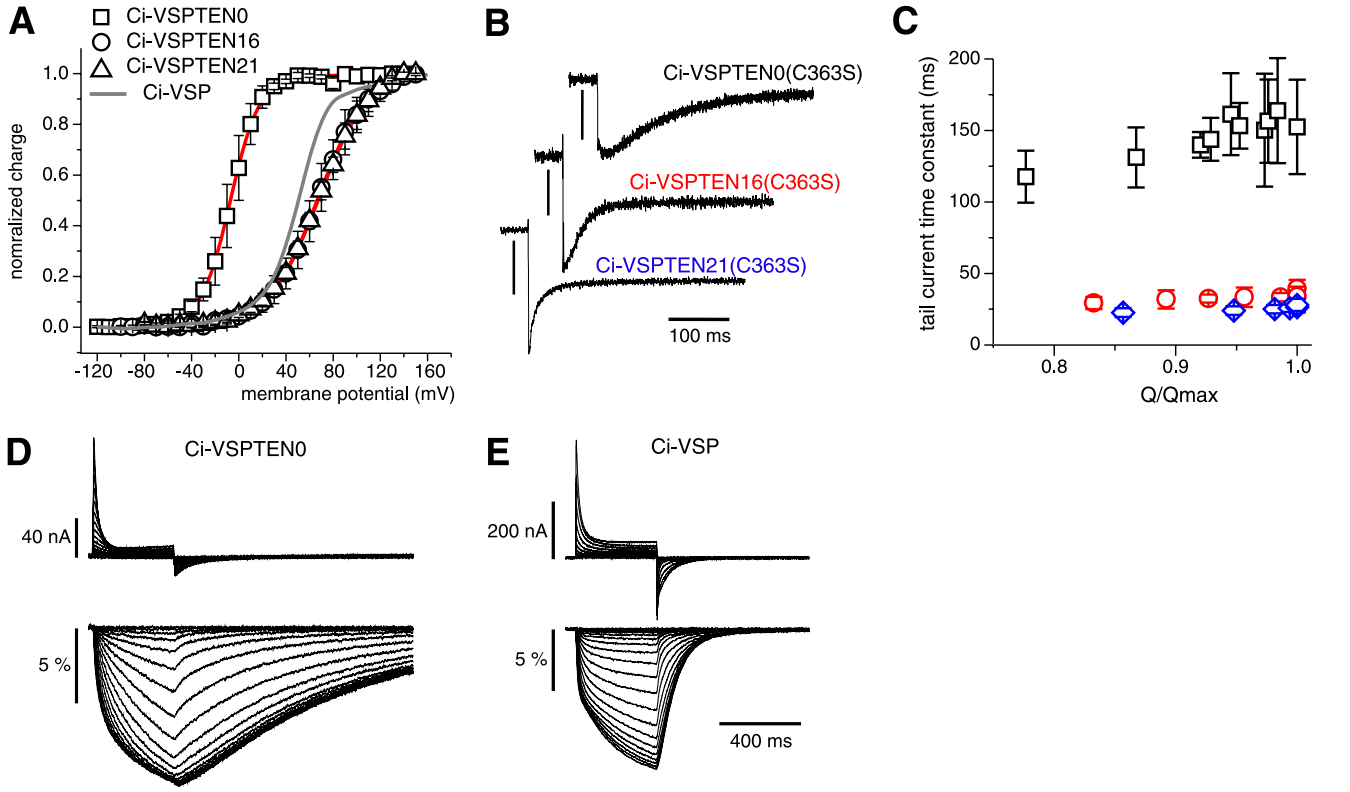

FIGURE 3. **Effect of the PBM on the voltage sensor dynamics.** *A*, voltage dependence of the sensing currents of the three Ci-VSPTEN chimeras were measured from *Xenopus* oocytes (27), using the catalytically inactive mutant C363S (equivalent to C124S in PTEN). Normalized *Q-V* curves were derived from the OFF sensing currents at −90 mV following a 400-ms step to the potentials indicated. The *gray* curve shows the voltage dependence of Ci-VSP-C363S recorded under the same conditions (27). Fits of a two-state Boltzmann distribution to the data (continuous red lines) yielded potentials at half-maximal charge transfer of −7 ± 0.2 mV ($n = 4$), +67 ± 0.4 mV ($n = 3$), and +69 ± 0.3 mV ($n = 4$), with charges of 2.0 ± 0.03 e_0, 1.2 ± 0.02 e_0 and 1.1 ± 0.01 e_0, for Ci-VSPTEN0, Ci-VSPTEN16, and Ci-VSPTEN21, respectively. *B*, OFF sensing currents of Ci-VSPTEN chimeras measured at −90 mV following a 400-ms test pulse to 0 mV for Ci-VSPTEN0 and +100 mV for Ci-VSPTEN16 and Ci-VSPTEN21. Current *scale bars*, 50 nA, 250 nA, and 100 nA, respectively. *C*, Weighted mean time constants of tail-sensing currents recorded as in *A* are shown for the nearly saturating region of the *Q-V* curves ($Q/Q_{max} > 0.75$; $n = 5$) for Ci-VSPTEN (*black*), Ci-VSPTEN16 (*red*), and Ci-VSPTEN21 (*blue*). *D* and *E*, sensing currents and changes in fluorescence intensity ($\Delta F/F_0$) from tetramethylrhodamine-5-maleimide-labeled Ci-VSPTEN0-G214C-C363S (*D*) and Ci-VSP-G214C-C363S (*E*) in response to depolarizing voltage steps (−120 to 140 mV).

specifically bind $PI(3,4,5)P_3$ and $PI(3,4)P_2$, respectively, Ci-VSPTEN16 evoked a decrease in membrane fluorescence upon depolarization (Fig. 2, *E* and *F*). Thus Ci-VSPTEN16 dephosphorylates both $PI(3,4,5)P_3$ and $PI(3,4)P_2$, consistent with the enzymatic activity of PTEN (Fig. 2*A*). Conversely, membrane fluorescence from the $PI(4,5)P_2$-specific probe, PLCδ1-PH-GFP (33), increased during depolarization (Fig. 2*G*). This result indicated production of $PI(4,5)P_2$ from $PI(3,4,5)P_3$ and confirmed that Ci-VSPTEN16 behaves as a 3′-phosphatase. Membrane association of PLCδ1-PH-GFP recovered rapidly following deactivation of Ci-VSPTEN, which most likely reflects rapid turnover of $PI(4,5)P_2$ (7, 34) and indicates that the $PI(4,5)P_2$ concentration is regulated independent of the $PI(3,4,5)P_3$ pool depleted by Ci-VSPTEN. Despite dephosphorylation of $PI(3,4)P_2$, membrane fluorescence of the PI(4)P specific probe OSBP-PH-GFP (35) seemed unaffected by depolarization (Fig. 2*H*), indicating the lack of substantial changes of the PI(4)P concentration by Ci-VSPTEN16 activation. However, this is expected, because the basal $PI(3,4)P_2$ content of the membrane is typically 1000-fold lower than its PI(4)P content (36). Based on these observations, we conclude that Ci-VSPTEN16 retains the enzymatic specificity of PTEN.

Role of PBM in Coupling Exogenous Enzymatic Activity to Voltage Sensor—To understand the coupling of catalytic activity to membrane potential, we next characterized the behavior of the VSD. Thus, we measured sensing currents from the chimeras carrying the mutation C363S expressed in *Xenopus* oocytes. Sensing currents are mainly produced by the movement of charged residues within the putative fourth trans-membrane segment (S4) of the VSD (5). The net sensing charge movement *versus* potential relationship (*Q-V* curve) revealed that both Ci-VSPTEN16 and -21 display voltage dependences similar to Ci-VSP (Fig. 3*A*). However, a shift to negative potentials was observed for Ci-VSPTEN0. In addition, Ci-VSPTEN0 displayed much slower OFF-sensing currents than Ci-VSPTEN16 and Ci-VSPTEN21 (Fig. 3, *B* and *C*). We further examined the movement of the S4 segment using voltage clamp fluorometry. Tetramethylrhodamine-5-maleimide was attached covalently to a cysteine replacing glycine 214 in the extracellular end of this segment, such that S4 movements result in fluorescence intensity changes (27, 37). Ci-VSP (Fig. 3*E*) and Ci-VSPTEN0 (Fig. 3*D*) displayed voltage-dependent fluorescence changes with strikingly different kinetics during repolarization: consistent

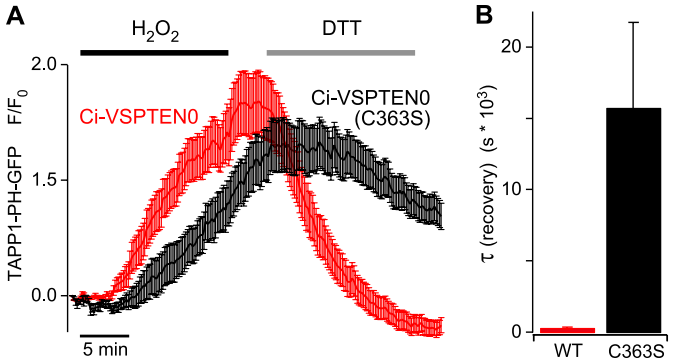

FIGURE 4. **Basal PI-3′-phosphatase activity of Ci-VSPTEN0 at resting membrane potential.** *A*, membrane association of the $PI(3,4)P_2$ probe TAPP1-PH-YFP in cells either coexpressing Ci-VSPTEN0 ($n = 47$ cells from nine independent experiments) or Ci-VSPTEN0 with the inactivating mutation C363S ($n = 35$ cells from 10 experiments) was imaged by TIRF microscopy. H_2O_2 (1 mM) was applied for 15 min, followed by application of DTT (5 mM) for 15 min as indicated. *B*, average time constants obtained from monoexponential fits to the signal recovery upon application of DTT from the same experiments shown in *A*. *Error bars* indicate S.E.

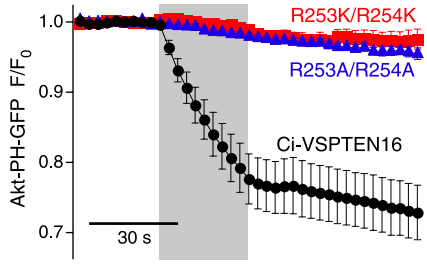

FIGURE 5. **Binding of the PBM is essential for phosphatase activation by the VSD.** Mutations that interfere with membrane binding of the PBM (R253A/R254A and R253K/R254K) abolish the depolarization-induced activation of enzymatic activity of Ci-VSPTEN16 as monitored by measuring membrane association of Akt-PH-GFP ($n = 7$ cells for each mutant). Experiments were done as described in the legend to Fig. 2, and data for Ci-VSPTEN16 are from Fig. 2*D* for comparison. The *gray* area indicates depolarization from −60 to +80 mV.

with sensing currents (*upper panels*), fluorescence signals (*lower panels*) were much slower for Ci-VSPTEN0.

Ci-VSPTEN0 Displays High Basal Activity—Despite an intact catalytic domain, Ci-VSPTEN0 produced no changes in membrane-associated fluorescence of Akt-PH-GFP during depolarization (data not shown). This might be a consequence of a strong negative shift in the voltage dependence of enzymatic activity in parallel with the voltage sensor behavior (Fig. 3*A*). Such a shift may render Ci-VSPTEN0 active at resting potential and thereby preclude additional depletion of $PI(3,4,5)P_3$ and $PI(3,4)P_2$ upon depolarization. However, we did not succeed in detecting depolarization-induced enzymatic activity even after prolonged hyperpolarization to abolish any activity present at resting membrane potential. We therefore tested for basal activity of Ci-VSPTEN0 under conditions of experimentally increased substrate concentration. To this end, cells were treated with H_2O_2, which is known to strongly increase the plasma membrane concentration of $PI(3,4)P_2$ (32, 38). The H_2O_2-triggered pathway leading to the $PI(3,4)P_2$ increase is not well understood but appears to involve the dysregulation of endogenous enzymes that otherwise control $PI(3,4)P_2$ levels, likely including inactivation of PTEN (32). It should be noted that H_2O_2 also inactivates PTEN, and consequently Ci-VSPTEN0, by formation of a disulfide bond between Cys^{71} and catalytic Cys^{124}, corresponding to Cys^{310} and Cys^{363} in the chimera (39). However, this inactivation is readily reversed in the presence of DTT (39). When H_2O_2 was applied to cells expressing Ci-VSPTEN0 and the $PI(3,4)P_2$ sensor TAPP1-PH, accumulation of $PI(3,4)P_2$ was readily detected as an increase in membrane association of TAPP-PH-GFP (Fig. 4*A*). Subsequent application of DTT to reverse oxidative inactivation induced a rapid decrease of membrane fluorescence in cells expressing Ci-VSPTEN0, indicating consumption of $PI(3,4)P_2$. In contrast, in cells expressing the inactive mutant Ci-VSPTEN0-C363S, recovery of $PI(3,4)P_2$ after H_2O_2 treatment was delayed and occurred much more slowly (Fig. 4*A*). Time constants obtained from monoexponential fits to the fluorescence decay upon application of DTT quantitatively confirmed the faster depletion of $PI(3,4)P_2$ with wild-type Ci-VSPTEN0 (Fig. 4*B*).

In conclusion, the fast removal of $PI(3,4)P_2$ upon treatment with DTT provides direct evidence for enzymatic activity of Ci-VSPTEN0 under basal conditions, *i.e.* at resting membrane potential. Additionally, the increase of $PI(3,4)P_2$ during H_2O_2 application was slightly stronger and faster in cells expressing Ci-VSPTEN0. This finding might be explained by a lower initial concentration of $PI(3,4)P_2$, which is again consistent with basal activity of Ci-VSPTEN0.

Mutations in PBM Abolished Ci-VSPTEN16 Activity—Both the effect of the PBM on the VSD movement (Fig. 3) and the differential enzymatic activity of Ci-VSPTEN16 *versus* Ci-VSPTEN0 are consistent with a pivotal role of the PBM in electrochemically coupling the exogenous enzymatic activity to the VSD movement. We directly tested this suggestion by introducing mutations that have been shown previously to affect the activity of PTEN, namely of $Arg^{14/15}$ of the PBM (15, 17). The corresponding amino acids ($Arg^{253/254}$) were also shown to be critical for electrochemical coupling of Ci-VSP (8, 24). Conversion of arginines Arg^{14}/Arg^{15} of the PBM to alanines or lysines completely abolished voltage-activated enzymatic activity of Ci-VSPTEN16 (Fig. 5), despite functionality of the VSD as confirmed by sensing currents (data not shown). This demonstrates functional uncoupling of the CD from the VSD, confirming the essential role of the PBM for activation of exogenous catalytic domains by a VSD.

Activation of Ci-VSPTEN16 in Intact Cells without Electrophysiological Instrumentation—So far, we have shown that Ci-VSPTEN allows the activation of PTEN enzymatic activity and the depletion of both $PI(3,4,5)P_3$ and $PI(3,4)P_2$ when used with electrophysiological single-cell techniques. Obviously, methods for controlling enzymatic activity with more general methods that can also be used on cell populations would substantially increase the range of potential applications.

We therefore explored K^+-induced depolarization as a means to activate Ci-VSPTEN16. Thus, we transiently depolarized the membrane potential by application of high extracellular K^+ concentration to otherwise undisturbed cells coexpressing Ci-VSPTEN16 and Akt-PH-GFP. K^+-induced depolarization triggered rapid depletion of both $PI(3,4,5)P_3$ and $PI(3,4)P_2$ as reported by translocation of Akt-PH-GFP from the

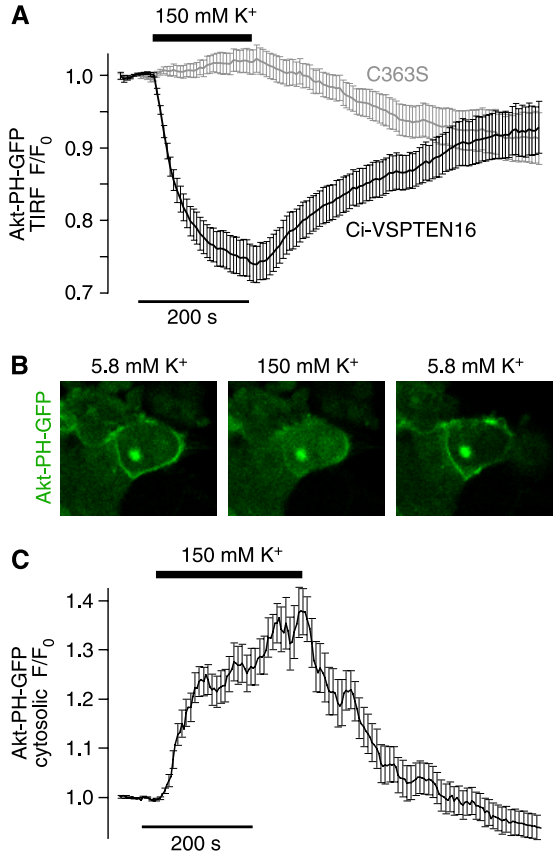

FIGURE 6. **Experimental control of Ci-VSPTEN activity in intact cells without use of electrophysiological instrumentation.** *A*, reversible dissociation of Akt-PH from the plasma membrane upon K^+-induced depolarization observed with Ci-VSPTEN16 ($n = 30$ cells from five independent experiments) but not with the catalytically inactive Ci-VSPTEN16-C363S ($n = 29$ cells, from five independent experiments), measured by TIRF microscopy. CHO cells were cotransfected with Ci-VSPTEN16, Akt-PH-GFP, PI3K, and the potassium channel TASK3. *B*, confocal images of OK cells show reversible translocation of Akt-PH from the plasma membrane to the cytosol upon K^+-induced depolarization. OK cells were cotransfected as described in *A*. *C*, averaged time course of K^+-induced translocation of Akt-PH-GFP obtained from experiments as described in *B* ($n = 19$ cells from two independent experiments).

membrane into the cytosol measured either by TIRF (Fig. 6*A*) or confocal microscopy (Fig. 6, *B* and *C*). Upon lowering the extracellular concentration of K^+ back to the initial condition, Akt-PH-GFP reassociated to the membrane, indicating resynthesis of $PI(3,4,5)P_3$ and $PI(3,4)P_2$. These results show that Ci-VSPTEN can be activated precisely and in a readily reversible manner by simply altering the extracellular concentration of K^+.

DISCUSSION

The recently discovered VSPs constitute a novel principle for the transduction of cellular electrical activity into intracellular biochemical signals, which differs fundamentally from the canonical principle for such transduction, *i.e.* influx of Ca^{2+} mediated by voltage-gated channels. Here, we explore molecular details of this novel principle and show that at least one exogenous enzyme can be operated by a voltage sensor domain. Specifically, fusing the VSD of Ci-VSP to PTEN, a key cytosolic modulator of intracellular signaling, yielded chimeric proteins that renders strictly voltage-dependent PTEN-like activity. To our knowledge, both Ci-VSPTEN16 and -21 represent the first example of conferring voltage control to a cytoplasmic enzyme, and they constitute the first generation of engineered VEnz.

Potential Applications for Engineered VEnz—We note that dramatically improving experimental control over PTEN activity provides a novel paradigm for the study of this important signaling enzyme. Stringent control of activity will enable addressing details of the enzymatic mechanism, cellular regulation, disease-causing mutations, and pharmacology of PTEN.

Beyond analysis of PTEN operation, voltage-controlled enzymes such as Ci-VSPTEN provide novel tools for analyzing cellular signaling. By inducing rapid phosphoinositide concentrations changes, Ci-VSPTEN can be used to probe the role and specificity of these messengers in many cellular processes and to analyze the timing of phosphoinositide signaling. Various methods have been used previously to address the roles of phosphoinositides in the control of cellular function. For example, overexpression and knockdown of enzymes involved in phosphoinositide synthesis or homeostasis have been used widely (40–42). Many fundamental cellular processes occurring at a variety of time scales are affected by phosphoinositides, including protein targeting, cell differentiation, and transcription. Therefore, with the above-mentioned methods, it may often be difficult to unequivocally define the direct role of these lipid messengers for the process under observation. Moreover, compensatory mechanisms may complicate the actual changes of phosphoinositide concentrations resulting from long term manipulation of synthesis or degradation (43). To overcome these problems, methods for triggered recruitment of enzymes and signaling molecules to the plasma membrane by rapamycin-induced dimerization have been developed (43, 44). Such recruitment has been used to induce rapid, albeit irreversible, alterations of phosphoinositide concentrations during experimental observation (43, 44).

Voltage-controlled activation of enzymes, as introduced here, takes this approach one step further by rapidly switching enzymatic activity "on" and "off." Thus, the precisely timed and reversible control of enzyme activation on a time scale of milliseconds provides a powerful tool for addressing temporal characteristics of signaling processes. Unlike the rapamycin-based approach, reversibility of activation allows the graded titration of phosphoinositide concentrations in the living cell (Fig. 2*D*) (7). Moreover, the recovery of phosphoinositide concentrations following a step-like perturbation (Fig. 2*C*) can yield unique insights into synthesis, homeostasis, and regulation of these messengers (7, 34). In analogy to Ci-VSPTEN, we envisage that fusion of different enzymatic domains to a VSD could provide novel tools for the temporally precise interference with diverse signaling pathways in the living cell, allowing for the experimental manipulation of cellular signaling networks beyond the level possible with the current cell biological or biochemical techniques.

Which enzymes or enzymatic domains may be amenable to functional coupling to VSDs? Here, we show that membrane binding of the PBM is critical for the activation of the exogenous enzymatic domain. The strong impact of the PBM on voltage sensor movement indicates that the VSD activates the exogenous enzyme by controlling the membrane binding of the PBM (see below), resembling electrochemical coupling in

native VSPs (8, 24). Although it has been shown that binding of the PBM to $PI(4,5)P_2$ increases the α-helicity of PTEN (22), it remains unknown whether activation occurs by the reorientation of the PD toward its membrane-resident substrate or by direct interaction of the PBM with the catalytic site. Although further work is needed to distinguish between these mechanisms, the latter model would suggest that generation of VEnz may be limited to CDs whose intrinsic activation mechanism involves a PBM-like motif. Such candidates may include, without being limited to, additional PTEN-related proteins, namely TPTE (45), TPIP (46), and PLIP (47). *In vitro*, these molecules may possess phosphoinositide phosphatase activities with distinct substrate specificities (46, 47). Generation of VEnz chimera with these proteins may substantially help to address their function in intact cells, which has been largely unexplored.

Mechanism of Coupling in Engineered VEnz—The loss of electrically triggered enzymatic activity observed with PBM mutants (Fig. 5) clearly demonstrates that electrochemical coupling in Ci-VSPTEN16 involves the PBM. How might the PBM mediate the interaction of VSD and PD? For PTEN, it has been shown that the PBM mediates both membrane binding and activation of catalytic activity (17, 19, 20). Likewise, work on Ci-VSP suggested that binding of the PBM to the plasma membrane is involved in coupling and that VSD movement modulates the PBM binding to control enzymatic activity (8, 24). Thus, sensor movement following depolarization is thought to promote membrane binding of the PBM and thereby activate the PBM. According to this model, the membrane binding of the PBM will reciprocally affect voltage sensor movement. Specifically, binding of the PBM upon depolarization will restrict subsequent voltage sensor movement upon repolarization, thus slowing down OFF sensing currents (8, 24).

Our present results with Ci-VSPTEN chimeras are consistent with this idea. Thus, mutations in the PBM most probably abrogate electrochemical coupling by interfering with membrane binding, similar to previous results obtained with Ci-VSP (8). We further observed that the full PBM from PTEN drastically slowed down voltage sensor return to the resting state upon repolarization, when compared with both of the other chimeras. According to the model outlined above, this observation suggests distinct membrane binding affinities of the different chimeric PBMs, with the full PBM of PTEN (*i.e.* Ci-VSPTEN0) exhibiting the strongest binding.

Following this idea, the proposed distinct membrane binding affinities may point to a specific interaction between the different PDs and their associated PBM. Thus, we note that the chimeric PBMs of Ci-VSPTEN16 and 21 yielded the fastest OFF-sensing currents, which may indicate that their bound conformation is less stable compared with native PBMs of Ci-VSP or Ci-VSPTEN0 associated with their original PDs (Fig. 3 and Ref. 8). These combined observations suggest that for optimal membrane binding, the PBM must match the catalytic domain with which they couple. In this view, the PBM in Ci-VSP serves as an adapter for the binding between the membrane and the CD. Combinatorial exchange of PBMs in VSP chimeras designed to operate as Ci-VSPTEN should help in directly addressing such specific interaction of PBM and PD.

One caveat to this model comes from its failure to fully explain the apparent lack of control of the VSD over the CD in Ci-VSPTEN0. The basal activity at negative potentials may either indicate that PTEN is constitutively active at all potentials (*i.e.* uncoupled from the VSD) or that the activation range is also shifted to negative potentials, as found for the sensing current. Both scenarios are not mutually exclusive and may be consistent with a higher membrane binding affinity of the PBM of PTEN. For the first case, it is plausible that the control of the VSD can be overridden by a strong interaction between the membrane and the PBM. For the second case, the shift in voltage dependence may prevent the sensor from adopting a conformation in which the PBM cannot bind (as in the case of Ci-VSPTEN16, -21 and other VSPs at negative potentials), resulting in high basal activity.

Furthermore, it should be noted that the observed shift in the voltage dependence of Ci-VSPTEN0 might be explained by an alternative scenario, in which the PBM influences the profile of the focused electrical field across the voltage sensor. In this case, the PBM could increase the sensitivity of the VSD to depolarization and therefore self-promote the activation of the catalytic activity, rendering a high basal activity. To distinguish between these different possibilities, further work is required, which is beyond the scope of the current study.

In Ci-VSP, cationic residues Arg^{245}, Arg^{246}, Arg^{253}, and Arg^{254} within the PBM are involved in electrochemical coupling, presumably by contributing to binding to negatively charged phospholipids in the membrane (8, 24). It is therefore remarkable that the PBM from PTEN, although lacking the positive charge at residue pair 245–246 (R245K-R246E; see Fig. 1*B*), produced slowed OFF-sensing currents and enhanced enzymatic activity at resting potentials, both consistent with enhanced membrane binding according to the coupling mechanism proposed above. This finding supports the idea that the PBM binds to membrane lipids in a stereo-specific manner rather than simply by electrostatic interaction with the membrane (8). This conclusion also is consistent with the elimination of electrochemical coupling by isocoulombic substitution of Arg^{253} and Arg^{254} to Lys (Fig. 5). Further detailed analysis of the role of individual residues within the PBM for membrane binding is required to fully resolve this issue.

In conclusion, we have been able to engineer a series of chimeric proteins conferring voltage sensitivity to the tumor suppressor PTEN *in vivo*. This work supports the idea that the PBM is a key element in the activation of VSP. In a broader view, this study constitutes a proof-of-concept to a novel approach for controlling enzymatic activity using VSDs.

Acknowledgments—We thank Drs. I. S. Ramsey, D. E. Logothetis, and L. J. DeFelice for helpful comments on the manuscript and S. Krieger and V. Petrou for excellent technical assistance. Constructs used in this work were kindly provided by Y. Okamura (Ci-VSP), T. Balla (PLCδ1-PH, Akt-PH, Btk-PH, OSBP-PH), D. Alessi (TAPP1-PH), J. Downward (PI3K), and J. Daut (TASK3).

REFERENCES

1. Finkbeiner, S., and Greenberg, M. E. (1998) *J. Neurobiol.* **37,** 171–189
2. Kingsbury, T. J., Bambrick, L. L., Roby, C. D., and Krueger, B. K. (2007)

J. Neurochem. **103,** 761–770
3. Wheeler, D. G., Barrett, C. F., Groth, R. D., Safa, P., and Tsien, R. W. (2008) *J. Cell Biol.* **183,** 849–863
4. Hossain, M. I., Iwasaki, H., Okochi, Y., Chahine, M., Higashijima, S., Nagayama, K., and Okamura, Y. (2008) *J. Biol. Chem.* **283,** 18248–18259
5. Murata, Y., Iwasaki, H., Sasaki, M., Inaba, K., and Okamura, Y. (2005) *Nature* **435,** 1239–1243
6. Murata, Y., and Okamura, Y. (2007) *J. Physiol.* **583,** 875–889
7. Halaszovich, C. R., Schreiber, D. N., and Oliver, D. (2009) *J. Biol. Chem.* **284,** 2106–2113
8. Villalba-Galea, C. A., Miceli, F., Taglialatela, M., and Bezanilla, F. (2009) *J. Gen. Physiol.* **134,** 5–14
9. Leslie, N. R., Batty, I. H., Maccario, H., Davidson, L., and Downes, C. P. (2008) *Oncogene* **27,** 5464–5476
10. Ooms, L. M., Horan, K. A., Rahman, P., Seaton, G., Gurung, R., Kethesparan, D. S., and Mitchell, C. A. (2009) *Biochem. J.* **419,** 29–49
11. Suh, B. C., and Hille, B. (2008) *Annu. Rev. Biophys.* **37,** 175–195
12. Cremona, O., Di Paolo, G., Wenk, M. R., Lüthi, A., Kim, W. T., Takei, K., Daniell, L., Nemoto, Y., Shears, S. B., Flavell, R. A., McCormick, D. A., and De Camilli, P. (1999) *Cell* **99,** 179–188
13. Haucke, V. (2005) *Biochem. Soc. Trans.* **33,** 1285–1289
14. Maehama, T., and Dixon, J. E. (1998) *J. Biol. Chem.* **273,** 13375–13378
15. Steck, P. A., Pershouse, M. A., Jasser, S. A., Yung, W. K., Lin, H., Ligon, A. H., Langford, L. A., Baumgard, M. L., Hattier, T., Davis, T., Frye, C., Hu, R., Swedlund, B., Teng, D. H., and Tavtigian, S. V. (1997) *Nat. Genet.* **15,** 356–362
16. Wymann, M. P., and Schneiter, R. (2008) *Nat. Rev. Mol. Cell Biol.* **9,** 162–176
17. Campbell, R. B., Liu, F., and Ross, A. H. (2003) *J. Biol. Chem.* **278,** 33617–33620
18. Das, S., Dixon, J. E., and Cho, W. (2003) *Proc. Natl. Acad. Sci. U.S.A.* **100,** 7491–7496
19. Vazquez, F., Matsuoka, S., Sellers, W. R., Yanagida, T., Ueda, M., and Devreotes, P. N. (2006) *Proc. Natl. Acad. Sci. U.S.A.* **103,** 3633–3638
20. Walker, S. M., Leslie, N. R., Perera, N. M., Batty, I. H., and Downes, C. P. (2004) *Biochem. J.* **379,** 301–307
21. Rahdar, M., Inoue, T., Meyer, T., Zhang, J., Vazquez, F., and Devreotes, P. N. (2009) *Proc. Natl. Acad. Sci. U.S.A.* **106,** 480–485
22. Redfern, R. E., Redfern, D., Furgason, M. L., Munson, M., Ross, A. H., and Gericke, A. (2008) *Biochemistry* **47,** 2162–2171
23. Liu, Y., and Bankaitis, V. A. (2010) *Prog. Lipid Res.* **49,** 201–217
24. Kohout, S. C., Bell, S. C., Liu, L., Xu, Q., Minor, D. L., Jr., and Isacoff, E. Y. (2010) *Nat. Chem. Biol.* **6,** 369–375
25. Iwasaki, H., Murata, Y., Kim, Y., Hossain, M. I., Worby, C. A., Dixon, J. E., McCormack, T., Sasaki, T., and Okamura, Y. (2008) *Proc. Natl. Acad. Sci. U.S.A.* **105,** 7970–7975
26. Lee, J. O., Yang, H., Georgescu, M. M., Di Cristofano, A., Maehama, T., Shi, Y., Dixon, J. E., Pandolfi, P., and Pavletich, N. P. (1999) *Cell* **99,** 323–334
27. Villalba-Galea, C. A., Sandtner, W., Starace, D. M., and Bezanilla, F. (2008) *Proc. Natl. Acad. Sci. U.S.A.* **105,** 17600–17607
28. Stefani, E., and Bezanilla, F. (1998) *Methods Enzymol.* **293,** 300–318
29. Cha, A., Zerangue, N., Kavanaugh, M., and Bezanilla, F. (1998) *Methods Enzymol.* **296,** 566–578
30. Schaechinger, T. J., and Oliver, D. (2007) *Proc. Natl. Acad. Sci. U.S.A.* **104,** 7693–7698
31. Denning, G., Jean-Joseph, B., Prince, C., Durden, D. L., and Vogt, P. K. (2007) *Oncogene* **26,** 3930–3940
32. Kimber, W. A., Trinkle-Mulcahy, L., Cheung, P. C., Deak, M., Marsden, L. J., Kieloch, A., Watt, S., Javier, R. T., Gray, A., Downes, C. P., Lucocq, J. M., and Alessi, D. R. (2002) *Biochem. J.* **361,** 525–536
33. Várnai, P., and Balla, T. (1998) *J. Cell Biol.* **143,** 501–510
34. Falkenburger, B. H., Jensen, J. B., and Hille, B. (2010) *J. Gen. Physiol.* **135,** 99–114
35. Balla, A., Tuymetova, G., Tsiomenko, A., Várnai, P., and Balla, T. (2005) *Mol. Biol. Cell* **16,** 1282–1295
36. Leslie, N. R., and Downes, C. P. (2002) *Cell Signal* **14,** 285–295
37. Kohout, S. C., Ulbrich, M. H., Bell, S. C., and Isacoff, E. Y. (2008) *Nat. Struct. Mol. Biol.* **15,** 106–108
38. Van der Kaay, J., Beck, M., Gray, A., and Downes, C. P. (1999) *J. Biol. Chem.* **274,** 35963–35968
39. Lee, S. R., Yang, K. S., Kwon, J., Lee, C., Jeong, W., and Rhee, S. G. (2002) *J. Biol. Chem.* **277,** 20336–20342
40. Chen, X., Talley, E. M., Patel, N., Gomis, A., McIntire, W. E., Dong, B., Viana, F., Garrison, J. C., and Bayliss, D. A. (2006) *Proc. Natl. Acad. Sci. U.S.A.* **103,** 3422–3427
41. Milosevic, I., Sørensen, J. B., Lang, T., Krauss, M., Nagy, G., Haucke, V., Jahn, R., and Neher, E. (2005) *J. Neurosci.* **25,** 2557–2565
42. Wang, Y. J., Li, W. H., Wang, J., Xu, K., Dong, P., Luo, X., and Yin, H. L. (2004) *J. Cell Biol.* **167,** 1005–1010
43. Varnai, P., Thyagarajan, B., Rohacs, T., and Balla, T. (2006) *J. Cell Biol.* **175,** 377–382
44. Suh, B. C., Inoue, T., Meyer, T., and Hille, B. (2006) *Science* **314,** 1454–1457
45. Tapparel, C., Reymond, A., Girardet, C., Guillou, L., Lyle, R., Lamon, C., Hutter, P., and Antonarakis, S. E. (2003) *Gene* **323,** 189–199
46. Walker, S. M., Downes, C. P., and Leslie, N. R. (2001) *Biochem. J.* **360,** 277–283
47. Pagliarini, D. J., Worby, C. A., and Dixon, J. E. (2004) *J. Biol. Chem.* **279,** 38590–38596
48. Lambert, C., Léonard, N., De Bolle, X., and Depiereux, E. (2002) *Bioinformatics* **18,** 1250–1256